

Dynamic analysis of functionally graded nanocomposite plates reinforced by wavy carbon nanotube

Rasool Moradi-Dastjerdi ^{*1} and Hamed Momeni-Khabisi ²

¹ Young Researchers and Elite Club, Khomeinishahr Branch, Islamic Azad University, Khomeinishahr, Iran

² Department of Mechanical Engineering, University of Jiroft, Jiroft, Iran

(Received February 09, 2016, Revised October 03, 2016, Accepted October 05, 2016)

Abstract. In this paper, free vibration, forced vibration, resonance and stress wave propagation behavior in nanocomposite plates reinforced by wavy carbon nanotube (CNT) are studied by a mesh-free method based on first order shear deformation theory (FSDT). The plates are resting on Winkler-Pasternak elastic foundation and subjected to periodic or impact loading. The distributions of CNTs are considered functionally graded (FG) or uniform along the thickness and their mechanical properties are estimated by an extended rule of mixture. In the mesh-free analysis, moving least squares (MLS) shape functions are used for approximation of displacement field in the weak form of motion equation and the transformation method is used for imposition of essential boundary conditions. Effects of CNT distribution, volume fraction, aspect ratio and waviness, and also effects of elastic foundation coefficients, plate thickness and time depended loading are examined on the vibrational and stresses wave propagation responses of the nanocomposite plates reinforced by wavy CNT.

Keywords: stress wave; resonance; vibration; nanocomposite plates; wavy carbon nanotube; mesh-free

1. Introduction

The two dimensional plate theories including classical plate theory (CPT), FSDT and the higher order shear deformation plate theories (HSDTs) are common for the analysis of plates. The classical plate theory, which neglects the transverse shear deformation effect, provides reasonable results for thin plates. It underestimates deflections and overestimates frequencies as well as buckling loads of moderately thick plate (Reddy 2004). So, many shear deformation plate theories which account for the transverse shear deformation effect have been developed for overcoming on the limitation of CPT. The Reissner (1945) and Mindlin (1951) theories are known as first order shear deformation plate theory. FSDT provides a sufficiently accurate description of response for thin to moderately thick plate (Thai and Choi 2012). The performance of the FSDT is strongly dependent on shear correction factors which are sensitive not only to the material and geometric properties but to the loading and boundary conditions. To avoid the use of shear correction factor and to include the actual cross-section warping of the plate, HSDTs have been extensively developed, considering the higher-order variation of in-plane displacement through the thickness (Reddy 1984).

*Corresponding author, Ph.D., E-mail: rasoul.moradi@iaukhsh.ac.ir

Iijima's works (Iijima 1991, Iijima *et al.* 1993) allowed to understand the great potentialities of Carbon Nanotubes and aroused the interest of many scientists, whose researches aimed to find a convenient application which was able to take advantage of them. Due to their excellent mechanical and thermal properties, CNTs have been seen immediately as the ideal candidate to reinforce those composite materials. So, these advantages increase using of carbon nanotube reinforced composites (CNTRCs) in engineering structures and technological fields, such as aerospace and mechanical engineering (Liew *et al.* 2015). Several important studies have focused on estimating the material properties of CNTRCs. These studies have proved that applying small amount of CNTs to the matrix can effectively enhance overall mechanical and electrical properties of polymeric composites (Selmi *et al.* 2007, Fidelus *et al.* 2005, Han and Elliott 2007). Martone *et al.* (2011) studied on the effects of CNT aspect ratio and waviness on the reinforcement behavior of CNT/epoxy composite. They revealed that progressive reduction of the tubes effective aspect ratio occurs because of the increasing connectedness between tubes upon an increase of their concentration. Also they investigated on the effect of nanotube curvature on the average contacts number between tubes by means of the waviness that accounts for the deviation from the straight particles assumption. Kundalwal and Ray (2013) studied on the effect of CNT waviness on the effective coefficient of thermal expansion of a continuous fuzzy fiber reinforced composite which is composed of carbon fibers, sinusoidally wavy CNTs and epoxy matrix by an analytical micromechanics model based on the method of cells approach.

On the other hand, mechanical properties of CNTRC will become worse if the volume fraction of CNTs arises beyond certain limit (Meguid and Sun 2004). Therefore, due to high cost of CNTs, in the modeling of CNTRC the concept of functionally graded materials (FGMs) might be incorporated to effectively make use of the CNTs. FGMs are classified as novel composite materials with gradient compositional variation. The concept of FGMs can be utilized for the management of a material's microstructure, so that the mechanical behavior of a structure made of such material can be improved. The composites, which are reinforced by CNTs with grading distribution, are called functionally graded carbon nanotube reinforced composites (FG-CNTRCs). By using their concept, several works on FG-CNTRC structures were carried out after the researches on the FGMs. Shen (2009) suggested that the interfacial bonding strength can be improved through the use of a graded distribution of CNTs in the matrix. He examined nonlinear bending behavior of FG-CNTRC plates and showed that the linear FG reinforcements can increase these mechanical behaviors. Yas and Sobhani Aragh (2010) used generalized differential quadrature (GDQ) method and 3D, linear and small strain elasticity theory to present free vibration behavior of simply supported rectangular continuously graded fiber reinforced (CGFR) plates resting on the Pasternak elastic foundations. Hedayati and Sobhani Aragh (2012) studied on the free vibration analysis of continuously graded CNTRC annular sectorial plates resting on Pasternak elastic foundation by 3D elasticity solution. Kaci *et al.* (2012) presented nonlinear cylindrical bending of simply supported FG-CNTRC plates subjected to uniform pressure loading in thermal environments. They reduced the governing equations to linear differential equation with nonlinear boundary conditions by a simple solution procedure. Sobhani Aragh *et al.* (2012) investigated the effect of CNT orientation on the natural frequencies characteristics of a continuously graded carbon nanotube-reinforced (CGCNTR) cylindrical panels based on the Eshelby–Mori–Tanaka approach and GDQ method. Zhu *et al.* (2012) studied on static and free vibration analyses of thin-to-moderately thick FG nanocomposite plates reinforced by straight CNTs. They developed a finite element method (FEM) based on the FSDT. Natarajan *et al.* (2014) investigated on the bending and free flexural vibration behavior of sandwich plates with CNT

reinforced composite face sheets based on higher-order structural theory. They reported that the deflection of sandwich plates decreases by increasing of CNT volume fraction. Kamarian *et al.* (2013) examined the vibrational behavior of FG-CNTRC plates resting on Winkler-Pasternak elastic foundation by Eshelby-Mori-Tanaka approach. Mehar *et al.* (2015) presented free vibration behavior of FG-CNTRC plates in thermal environment by an FEM based on HSDT. Ansari *et al.* (2015) investigated nonlinear forced vibration behavior of FG-CNTRC plates using of FSDT and von Karman-type kinematic relations. They used GDQ method and a Galerkin based scheme to obtain a time-varying set of ordinary differential equations of Duffing-type. Fan and Wang (2016) investigated the effect of matrix cracks on the nonlinear bending and thermal postbuckling of a piezoelectric shear deformable laminated beam which contains both CNTRC layers and piezoelectric fiber reinforced composite (PFRC) layers. They assumed the beam resting on a two-parameter elastic foundation in thermal environments and used von Kármán nonlinear strain-displacement relationships and HSDT. Also, The effect of CNT agglomeration on the stresses due to bending behavior of FG-CNTRC open cylindrical shells (Jafari Mehrabadi and Sobhani Aragh 2014), and also on the vibration behavior of arbitrary shaped plate (Fantuzzi *et al.* 2016), conical shells (Kamarian *et al.* 2016) and laminated composite doubly-curved shells (Tornabene *et al.* 2016) are presented.

Furthermore, there are some investigations to analysis of FG-CNTRC and FGM structures which used some forms of mesh-free method were used. Qian *et al.* (2004) examined the static and vibrational behaviors of a thick rectangular FGM plate by a meshless local Petrov–Galerkin (MLPG) method based on a higher order shear and normal deformable plate theory. Moradi-Dastjerdi *et al.* (2013a, b) studied on the static and dynamic responses of FG nanocomposite cylinders reinforced by straight CNTs. They used a mesh-free method based on MLS shape function. The element-free *kp*-Ritz method based on FSDT is used by Lei *et al.* (2013a, b) for buckling and free vibration analyses of FG-CNTRC plates. Ansari and Arjangpay (2014) presented axial buckling and free vibration characteristics of SWCNTs with different boundary conditions by MLPG method. They used a nonlocal shell model accounting for the small scale effect and showed that the critical axial buckling loads and natural frequencies of SWCNTs are strongly dependent on the small scale effect and geometrical parameters. Zhang *et al.* (2015a, b) used an element-free based improved moving least squares-Ritz (IMLS-Ritz) method and FSDT to study the buckling behavior FG-CNTRC plates resting on Winkler foundations and nonlinear bending of these plates resting on Pasternak elastic foundation. Also, dynamic stability analysis of FG-CNTRC cylindrical panels under static and periodic axial force is presented by using the element-free *kp*-Ritz method (Lei *et al.* 2016). Moradi-Dastjerdi (2016) presented the effects of CNT orientation and aggregation on the stress wave propagation of FG-CNTRC cylinders by the same mesh-free method.

But in all the above mentioned works about FG-CNTRC structures, it can be seen that they assumed that CNTs are straight and didn't consider the effects of CNT aspect ratio and waviness while, CNT curvature (waviness index) dramatically decreases modulus of elasticity. But, Jam *et al.* (2012) investigated the effects of CNT aspect ratio and waviness on the vibrational behavior of nanocomposite cylindrical panels. They used a 3D elasticity theory and indicated that CNTs volume fraction and distribution pattern have a significant effect on the natural frequencies of a nanocomposite cylindrical panel. Also, Moradi-Dastjerdi *et al.* (2014) studied on the effects of CNTs waviness and aspect ratio on the vibrational and dynamic behaviors of FG-CNTRC cylinders by a mesh-free method. They showed that CNT waviness has a significant effect on the natural frequency and stress wave propagation of nanocomposite cylinders reinforced by wavy

CNTs. Finally, the effects of CNT waviness and aspect ratio on the buckling behavior of FG-CNTRC plates subjected to in-plane loads are investigated by Shams *et al.* (2015). They used reproducing kernel particle method (RKPM) based on modified FSDT.

In this paper, vibrational, resonance and dynamic behaviors of nanocomposite plates reinforced by wavy CNTs resting on two parameter elastic foundation are investigated by a mesh-free method based on FSDT. The plates are subjected to periodic or impact loads for vibration or wave propagation analysis, respectively. In the mesh-free method, MLS shape functions are used to approximate of displacement field in the weak form of motion equation and for imposition of essential boundary conditions, the transformation method is used. This mesh-free method doesn't increase the calculations against Element-Free Galerkin (EFG). A micro mechanical model is used to estimate material properties of FG-CNTRC plates but for the scale difference between the nano and micro levels, some efficiency parameters are defined and estimated by matching the Young's moduli of CNTRCs obtained by the extended rule of mixture to those obtained by MD simulation. CNTs volume fraction of nanotube is assumed functionally graded along the plate thickness. So the effect of CNT distribution and the effects of aspect ratio, waviness and volume fraction of CNTs, and geometric dimension elastic foundation coefficients of plates are investigated on the free vibration, forced vibration, resonance behavior and stress wave propagation of the functionally graded composite plates reinforced by wavy CNTs.

2. Material properties in FG-CNTRC plates

In this paper, FG-CNTRC plates resting on Winkler-Pasternak elastic foundation are considered with length a , width b , and thickness h , as shown in Fig. 1. Volume fraction of CNT is assumed to be graded along the plate thickness. The plates are made from a mixture of wavy SWCNTs and isotropic matrix. The wavy SWCNT reinforcement is either uniformly distributed (UD) or functionally graded in the plate thickness. To obtain mechanical properties of CNT/polymer composites an extended rule of mixture equation assumes that the fibers are wavy and has uniform dispersion in the polymer matrix. This equation can't consider the length of fiber, so it can be modified by incorporating efficiency parameter (η^*) to account the nanotube aspect ratio (AR) and waviness (w) (Martone *et al.* 2011). The effective mechanical properties of the CNTRC plates are obtained based on a micromechanical model according to Shen (2009)

$$E_1 = \eta_1 V_{CN} E_{1,\eta^*} + V_m E^m \quad (1)$$

$$\frac{\eta_2}{E_2} = \frac{V_{CN}}{E_{2,\eta^*}} + \frac{V_m}{E^m} \quad (2)$$

$$\frac{\eta_3}{G_{12}} = \frac{V_{CN}}{G_{12,\eta^*}} + \frac{V_m}{G^m} \quad (3)$$

$$\nu_{ij} = V_{CN} \nu_{ij}^{CN} + V_m \nu^m \quad i, j = 1, 2, 3 \quad \text{and} \quad i \neq j \quad (4)$$

$$\rho = V_{CN} \rho^{CN} + V_m \rho^m \quad (5)$$

where

$$E_{i,\eta^*} = \eta^* E_i^{CN} \tag{6}$$

$$\eta^* = 1 - \frac{\tanh(K \cdot AR / (1 + \langle c \rangle))}{K \cdot AR / (1 + \langle c \rangle)}, \quad K = \sqrt{\frac{-2}{1 + \nu_m} \left/ \left(\frac{E^{CN}}{E^m} \ln(V_{CN}) \right) \right.} \tag{7}$$

and where E_i^{CN} , G_{12}^{CN} , ν^{CN} , E_{η^*} , $\langle c \rangle$ and ρ^{CN} are elasticity modulus, shear modulus, Poisson's ratio, effective reinforcement modulus, the average number of contacts per particle and density, respectively, of the carbon nanotube. E^m , G^m , ν^m and ρ^m are corresponding properties for the matrix. V_{CN} and V_m are the fiber (CNT) and matrix volume fractions and are related by $V_{CN} + V_m = 1$. η_j ($j = 1, 2, 3$) are the CNT efficiency parameters and they can be computed by matching the elastic modulus of CNTRCs observed from the molecular dynamic (MD) simulation result with the numerical results obtained from the extended rule of mixture in Eqs. (1)-(5). It must be noticed that the average number of contacts, $\langle c \rangle$, for tubes is dependent on their aspect ratio (Martone *et al.* 2011)

$$\langle c \rangle = w V_{CN} \left(4 + \frac{3AR^2}{3AR + 2} \right) \tag{8}$$

where the waviness index, w , has been introduced in order to account the CNTs curvature within the real composite. Accordingly to Martone *et al.* (2011), the variation of the excluded volume due to nanotubes curvature has been here investigated by introducing the waviness parameter, w .

The variation profile of CNT volume fraction along the plate thickness has important effects on the plate behavior. In this paper, three linear types (FG-V, FG-X and FG-O) are assumed for the distribution of CNT reinforcements along the thickness direction in FG-CNTRC plates. Also, a uniform distribution for CNTs in the nanocomposite plate with the same thickness, referred to as UD-CNTRC, is considered as a comparator. These distributions along the thickness are shown in Fig. 2, where

$$V_{CN}^* = \frac{\rho^m}{\rho^m + (\rho^{CN} / w^{CN}) - \rho^{CN}} \tag{9}$$

and w^{CN} is the mass fraction of nanotube.

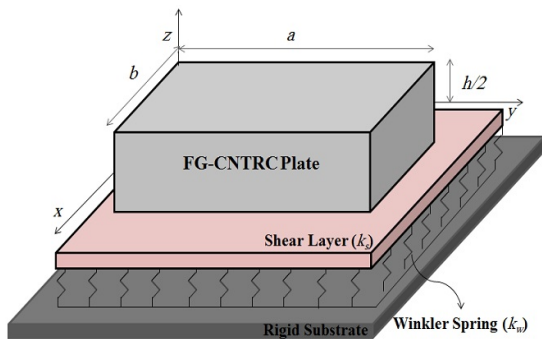


Fig. 1 Schematic of the plate resting on Winkler-Pasternak elastic foundation

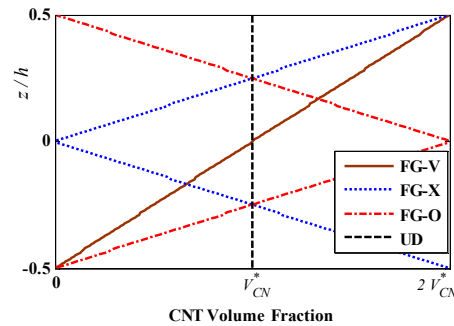


Fig. 2 Variation of V_{CN} along the thickness of plate for different CNT distributions

3. Governing equations

Based on the FSDT, the displacement components can be defined as (Reddy 2004)

$$\begin{aligned} u(x, y, z) &= u_0(x, y) + z\theta_x(x, y) \\ v(x, y, z) &= v_0(x, y) + z\theta_y(x, y) \\ w(x, y, z) &= w_0(x, y) \end{aligned} \quad (10)$$

where u , v and w are displacements in the x , y , z directions, respectively. u_0 , v_0 and w_0 denote mid-plane displacements, θ_x and θ_y rotations of normal to the mid-plane about y -axis and x -axis, respectively. The kinematic relations can be obtained as follows

$$\begin{Bmatrix} \varepsilon_{xx} \\ \varepsilon_{yy} \\ \gamma_{xy} \end{Bmatrix} = \boldsymbol{\varepsilon}_0 + z\boldsymbol{\kappa}, \quad \begin{Bmatrix} \gamma_{yz} \\ \gamma_{xz} \end{Bmatrix} = \boldsymbol{\gamma}_0 \quad (11)$$

where

$$\begin{aligned} \boldsymbol{\varepsilon}_0 &= \begin{Bmatrix} \partial u_0 / \partial x \\ \partial v_0 / \partial y \\ \partial u_0 / \partial y + \partial v_0 / \partial x \end{Bmatrix}, \quad \boldsymbol{\kappa} = \begin{Bmatrix} \partial \theta_x / \partial x \\ \partial \theta_y / \partial y \\ \partial \theta_x / \partial y + \partial \theta_y / \partial x \end{Bmatrix}, \\ \boldsymbol{\gamma}_0 &= \begin{Bmatrix} \partial v / \partial z + \partial w / \partial y \\ \partial u / \partial z + \partial w / \partial x \end{Bmatrix} = \begin{Bmatrix} \varphi_y + \partial w_0 / \partial y \\ \varphi_x + \partial w_0 / \partial x \end{Bmatrix} \end{aligned} \quad (12)$$

The linear constitutive relations of a FG plate can be written as

$$\begin{aligned} \begin{Bmatrix} \sigma_x \\ \sigma_y \\ \sigma_{xy} \end{Bmatrix} &= \begin{bmatrix} Q_{11}(z) & Q_{12}(z) & 0 \\ Q_{12}(z) & Q_{22}(z) & 0 \\ 0 & 0 & Q_{66}(z) \end{bmatrix} \begin{Bmatrix} \varepsilon_x \\ \varepsilon_y \\ \varepsilon_{xy} \end{Bmatrix} \text{ or } \boldsymbol{\sigma} = \mathbf{Q}_b \boldsymbol{\varepsilon} \\ \begin{Bmatrix} \sigma_{yz} \\ \sigma_{xz} \end{Bmatrix} &= \alpha(z) \begin{bmatrix} Q_{44}(z) & 0 \\ 0 & Q_{55}(z) \end{bmatrix} \begin{Bmatrix} \varepsilon_{yz} \\ \varepsilon_{xz} \end{Bmatrix} \text{ or } \boldsymbol{\tau} = \alpha(z) \mathbf{Q}_s \boldsymbol{\gamma} \end{aligned} \quad (13)$$

in which α denotes the transverse shear correction coefficient, which is suggested as $\alpha = 5 / 6$ for homogeneous materials. For FGMs, the shear correction coefficient is taken to be $\alpha = 5 / (6 - (v_{CN}V_{CN} + v_mV_m))$ (Efraim and Eisenberger 2007). Also where

$$\begin{aligned} Q_{11} &= \frac{1 - \nu_{23}(z)\nu_{32}(z)}{E_2(z)E_3(z)\Delta(z)}, \quad Q_{22} = \frac{1 - \nu_{31}(z)\nu_{13}(z)}{E_1(z)E_3(z)\Delta(z)}, \quad Q_{12} = \frac{\nu_{21}(z) + \nu_{31}(z)\nu_{23}(z)}{E_2(z)E_3(z)\Delta(z)} \\ Q_{44} &= G_{23}(z), \quad Q_{55} = G_{31}(z), \quad Q_{66} = G_{12}(z) \end{aligned} \quad (14)$$

$$\Delta = \frac{1 - \nu_{32}(z)\nu_{23}(z) - \nu_{21}(z)\nu_{12}(z) - \nu_{13}(z)\nu_{31}(z) - 2\nu_{32}(z)\nu_{21}(z)\nu_{13}(z)}{E_1(z)E_2(z)E_3(z)} \quad (14)$$

Also by considering of the Pasternak foundation model, total energy of the plate is as

$$U = \frac{1}{2} \int_V [\boldsymbol{\varepsilon}^T \boldsymbol{\sigma} + \boldsymbol{\gamma}^T \boldsymbol{\tau} - \rho(z)(\dot{u}^2 + \dot{v}^2 + \dot{w}^2)] dV + \frac{1}{2} \int_A [k_w w^2 + k_s \left[\left(\frac{\partial w}{\partial x} \right)^2 + \left(\frac{\partial w}{\partial y} \right)^2 \right]] dA + \int_A [P(t)w] dA \quad (15)$$

where $P(t)$ is the time depend applied load, k_w and k_s are coefficients of Winkler and Pasternak (shear) foundation. If the foundation is modeled as the linear Winkler foundation, the coefficient k_s in Eq. (15) is zero.

4. Mesh-free numerical analysis

In these analyses moving least square shape functions introduced by Lancaster and Salkauskas (1981) is used for approximation of displacement vector in the weak form of motion equation. Displacement vector \mathbf{d} can be approximated by MLS shape functions as follows

$$\hat{\mathbf{d}} = \sum_{i=1}^N \phi_i d_i \quad (16)$$

where N is the total number of nodes, $\hat{\mathbf{d}}$ is virtual nodal values vector and ϕ_i is MLS shape function of node located at $X(x, y) = X_i$ and they are defined as follows

$$\hat{\mathbf{d}} = [\hat{u}_i, \hat{v}_i, \hat{w}_i, \hat{\theta}_{x_i}, \hat{\theta}_{y_i}]^T \quad (17)$$

and

$$\phi_i(\mathbf{X}) = \underbrace{\mathbf{P}^T(\mathbf{X})[\mathbf{H}(\mathbf{X})]^{-1}W(\mathbf{X} - \mathbf{X}_i)\mathbf{P}(\mathbf{X}_i)}_{(1 \times 1)} \quad (18)$$

In the above equation, W is cubic Spline weight function, \mathbf{P} is base vector and \mathbf{H} is moment matrix and are defined as follows

$$\mathbf{P}(\mathbf{X}) = [1, x, y]^T \quad (19)$$

$$\mathbf{H}(\mathbf{X}) = \left[\sum_{i=1}^n W(\mathbf{X} - \mathbf{X}_i) \mathbf{P}(\mathbf{X}_i) \mathbf{P}^T(\mathbf{X}_i) \right] \quad (20)$$

By using of the MLS shape function, Eq. (11) can be written as

$$\boldsymbol{\varepsilon} = \mathbf{B}_m \hat{\mathbf{d}} + z \mathbf{B}_b \hat{\mathbf{d}} \quad , \quad \boldsymbol{\gamma} = \mathbf{B}_s \hat{\mathbf{d}} \quad (21)$$

in which

$$\mathbf{B}_m = \begin{bmatrix} \phi_{i,x} & 0 & 0 & 0 & 0 \\ 0 & \phi_{i,y} & 0 & 0 & 0 \\ \phi_{i,y} & \phi_{i,x} & 0 & 0 & 0 \end{bmatrix}, \mathbf{B}_b = \begin{bmatrix} 0 & 0 & 0 & \phi_{i,x} & 0 \\ 0 & 0 & 0 & 0 & \phi_{i,y} \\ 0 & 0 & 0 & \phi_{i,y} & \phi_{i,x} \end{bmatrix} \quad (22)$$

$$\mathbf{B}_s = \begin{bmatrix} 0 & 0 & \phi_{i,x} & \phi_i & 0 \\ 0 & 0 & \phi_{i,y} & 0 & \phi_i \end{bmatrix}$$

Also for elastic foundation, $\boldsymbol{\varphi}_w$ and \mathbf{B}_p can be defined as following

$$\boldsymbol{\varphi}_w = [0 \quad 0 \quad \phi_i \quad 0 \quad 0], \mathbf{B}_p = \begin{bmatrix} 0 & 0 & \phi_{i,x} & 0 & 0 \\ 0 & 0 & \phi_{i,y} & 0 & 0 \end{bmatrix} \quad (23)$$

Substitution of Eqs. (13) and (21) in Eq. (15) leads to

$$U = \frac{1}{2} \int_A \int_z \hat{\mathbf{d}}^T \left[\mathbf{B}_m^T \mathbf{A} \mathbf{B}_m + \mathbf{B}_m^T \bar{\mathbf{B}} \mathbf{B}_b + \mathbf{B}_b^T \bar{\mathbf{B}} \mathbf{B}_m + \mathbf{B}_b^T \mathbf{D} \mathbf{B}_b + \mathbf{B}_s^T \mathbf{A}_s \mathbf{B}_s \right] dz \hat{\mathbf{d}} dA \quad (24)$$

$$- \frac{1}{2} \int_A \int_z \hat{\mathbf{d}}^T \left[\mathbf{G}_i^T \bar{\mathbf{M}} \mathbf{G}_j \right] dz \hat{\mathbf{d}} dA + \frac{1}{2} \int_A \left[\boldsymbol{\varphi}_w^T k_w \boldsymbol{\varphi}_w + \mathbf{B}_p^T k_s \mathbf{B}_p \right] \hat{\mathbf{d}} dA + \frac{1}{2} \int_A \boldsymbol{\varphi}_w^T P(t) dA$$

in which the components of the extensional stiffness \mathbf{A} , bending-extensional coupling stiffness $\bar{\mathbf{B}}$, bending stiffness \mathbf{D} , transverse shear stiffness \mathbf{A}_s and also \mathbf{G}_i and $\bar{\mathbf{M}}$ are introduced for mass matrix and they are defined as

$$(\mathbf{A}, \bar{\mathbf{B}}, \mathbf{D}) = \int_{-h/2}^{h/2} \mathbf{Q}_b(1, z, z^2) dz, \quad \mathbf{A}_s = \alpha \int_{-h/2}^{h/2} \mathbf{Q}_s dz \quad (25)$$

and

$$\mathbf{G}_i = \begin{bmatrix} \phi_i & 0 & 0 & 0 & 0 \\ 0 & \phi_i & 0 & 0 & 0 \\ 0 & 0 & \phi_i & 0 & 0 \\ 0 & 0 & 0 & \phi_i & 0 \\ 0 & 0 & 0 & 0 & \phi_i \end{bmatrix}, \bar{\mathbf{M}} = \begin{bmatrix} I_0 & 0 & 0 & I_1 & 0 \\ 0 & I_0 & 0 & 0 & I_1 \\ 0 & 0 & I_0 & 0 & 0 \\ I_1 & 0 & 0 & I_2 & 0 \\ 0 & I_1 & 0 & 0 & I_2 \end{bmatrix} \quad (26)$$

where I_0 , I_1 and I_2 are the normal, coupled normal-rotary and rotary inertial coefficients, respectively and defined by

$$(I_0, I_1, I_2) = \int_{-h/2}^{h/2} \rho(z)(1, z, z^2) dz \quad (27)$$

It can be noticed that the arrays of bending-extensional coupling stiffness matrix, $\bar{\mathbf{B}}$, are zero for symmetric laminated composites. Finally, by a derivative with respect to displacement vector,

$\hat{\mathbf{d}}$, the Eq. (24) can be expressed as

$$\mathbf{M}\ddot{\hat{\mathbf{d}}} + \mathbf{K}\hat{\mathbf{d}} = \mathbf{F} \tag{28}$$

in which, \mathbf{M} , \mathbf{K} and \mathbf{F} are mass matrix, stiffness matrix and force vector, respectively and are defined as

$$\mathbf{M} = \int_A \mathbf{G}_i^T \overline{\mathbf{M}} \mathbf{G}_j dA \tag{29}$$

$$\mathbf{K} = \mathbf{K}_m + \mathbf{K}_b + \mathbf{K}_s + \mathbf{K}_w + \mathbf{K}_p \tag{30}$$

$$\mathbf{F} = \int_A \boldsymbol{\phi}_w^T P(t) dA \tag{31}$$

in which, \mathbf{K}_m , \mathbf{K}_b and \mathbf{K}_s are stiffness matrixes of extensional, bending-extensional and bending, respectively and also, \mathbf{K}_w and \mathbf{K}_p are stiffness matrixes that represented the Winkler and Pasternak elastic foundations. They are defined as

$$\mathbf{K}_m = \int_A \left[\mathbf{B}_m^T \mathbf{A} \mathbf{B}_m + \mathbf{B}_m^T \overline{\mathbf{B}} \mathbf{B}_b + \mathbf{B}_b^T \overline{\mathbf{B}} \mathbf{B}_m \right] dA, \mathbf{K}_b = \int_A \mathbf{B}_b^T \mathbf{D} \mathbf{B}_b dA, \mathbf{K}_s = \int_z \mathbf{B}_s^T \mathbf{A}_s \mathbf{B}_s dA \tag{32}$$

$$\mathbf{K}_w = \int_A \boldsymbol{\phi}_w^T k_w \boldsymbol{\phi}_w dA, \mathbf{K}_p = \int_A \mathbf{B}_p^T k_s \mathbf{B}_p dA \tag{33}$$

For numerical integration, problem domain is discretized to a set of background cells with gauss points inside each cell. Then global stiffness matrix \mathbf{K} is obtained numerically by sweeping all gauss points. Imposition of essential boundary conditions in the system of Eq. (28) is not possible. Because MLS shape functions don't satisfy the Kronecker delta property. In this work transformation method is used for imposition of essential boundary conditions. For this purpose transformation matrix is formed by establishing relation between nodal displacement vector \mathbf{d} and virtual displacement vector $\hat{\mathbf{d}}$.

$$\mathbf{d} = \mathbf{T}\hat{\mathbf{d}} \tag{34}$$

\mathbf{T} is the transformation matrix that is a $(5N \times 5N)$ matrix and is defined as

$$\mathbf{T} = \begin{bmatrix} \phi_1(x_1) \times \mathbf{I}_{(5 \times 5)} & \phi_1(x_2) \times \mathbf{I}_{(5 \times 5)} & \dots & \phi_1(x_N) \times \mathbf{I}_{(5 \times 5)} \\ \phi_2(x_1) \times \mathbf{I}_{(5 \times 5)} & \phi_2(x_2) \times \mathbf{I}_{(5 \times 5)} & \dots & \phi_2(x_N) \times \mathbf{I}_{(5 \times 5)} \\ \vdots & \vdots & \ddots & \vdots \\ \phi_N(x_1) \times \mathbf{I}_{(5 \times 5)} & \phi_N(x_2) \times \mathbf{I}_{(5 \times 5)} & \dots & \phi_N(x_N) \times \mathbf{I}_{(5 \times 5)} \end{bmatrix} \tag{35}$$

where $\mathbf{I}_{(5 \times 5)}$ is an identity matrix of size 5. By using Eq. (34), system of linear Eq. (28) can be rearranged to

$$\hat{\mathbf{M}}\ddot{\mathbf{d}} + \hat{\mathbf{K}}\mathbf{d} = \hat{\mathbf{F}} \tag{36}$$

where

$$\hat{\mathbf{M}} = \mathbf{T}^{-T} \mathbf{M} \mathbf{T}^{-1} \quad , \quad \hat{\mathbf{K}} = \mathbf{T}^{-T} \mathbf{K} \mathbf{T}^{-1} \quad , \quad \hat{\mathbf{F}} = \mathbf{T}^{-T} \mathbf{F} \quad (37)$$

Now the essential B. Cs. can be enforced to the modified equations system Eq. (36) easily like the finite element method. By using of Newmark method, the time depended system Eq. (36) can be solved and time history of displacement can be derived. Also, in the absence of external forces, Eq. (36) is simplified as follows

$$\hat{\mathbf{M}} \ddot{\mathbf{d}} + \hat{\mathbf{K}} \mathbf{d} = 0 \quad (38)$$

So, natural frequencies and mode shapes of the sandwich plate are determined by solving this eigenvalue problem.

5. Results and discussions

In this section, vibrational and dynamic behaviors of functionally graded wavy CNT-reinforced nanocomposite plates are investigated using the mesh-free method. The Poly (methyl-methacrylate), referred as PMMA, is selected as the matrix with isotropic material properties. The relevant material properties for CNTs and PMMA are as follows (Shen 2009):

$$E^m = 2.5 \text{ GPa}, \quad \rho^m = 1150 \text{ Kg/m}^3 \quad \text{and} \quad \nu^m = 0.34 \quad \text{for PMMA}$$

$E_1^{CN} = 5.6466 \text{ TPa}$, $E_2^{CN} = 7.0800 \text{ TPa}$, $G_{12}^{CN} = 1.9445 \text{ TPa}$, $\rho^{CN} = 1400 \text{ Kg/m}^3$ and $\nu_{12}^{CN} = 0.175$ for (10,10) SWCNTs and material properties of the nanocomposite are derived from Eqs. (1)-(5) and with respect to $\eta_3 = 0.7\eta_2$ (Song and Youn 2006) and values of Table 1 (Moradi-Dastjerdi *et al.* 2013b). The accuracy of this method has been investigated by a **comparing with experimental** results (Jam *et al.* 2012, Moradi-Dastjerdi *et al.* 2014, and Moradi-Dastjerdi Pourasghar 2016).

In this work, free vibration, forced vibration, resonance phenomenon and stress wave propagation are presented to investigate the mechanical characteristics of FG-CNTRC plates by several numerical examples. The plates are assumed subjected to periodic or impact load and resting on Winkler-Pasternak elastic foundation. At first, convergence and accuracy of the mesh-free method are examined by a comparison between the results and reported results in literatures about homogeneous, FGM and straight CNT-reinforced composite plates. Then, new mesh-free results on the vibrational and dynamic characteristics of wavy CNT-reinforced composite plates on the elastic foundation will report. In all examples of CNTRC plates, the foundation parameters are presented in the non-dimensional form of $K_w = k_w a^4 / D$ and $K_s = k_s a^2 / D$, in which $D = E_m h^3 / 12(1 - \nu_m^2)$ is a reference bending rigidity of the plate. Also, the normalized deflection and natural frequency of the applied plates are defined as (Ferreira *et al.* 2009)

$$\hat{q} = 10 E_m h^3 q / P_0 a^4 \quad (39)$$

$$\hat{\omega} = \omega h \sqrt{\rho_m / E_m} \quad (40)$$

in which, f_0 is the value of amplitude of time depended applied load and q is central deflection.

5.1 Validation models

The convergence of applied mesh-free method is examined in Fig. 3. Consider a simply

Table 1 Efficiency parameter of (10,10) SWCNT at $T_0 = 300$ K (Martone *et al.* 2011)

V_{CN}^*	η_1	η_2
0.12	0.137	1.022
0.17	0.142	1.626
0.28	0.141	1.585

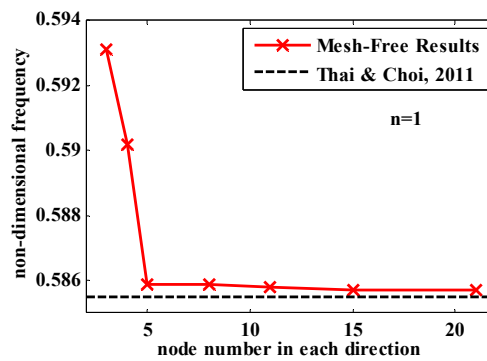


Fig. 3 Convergence of the non-dimensional fundamental frequency, $\hat{\omega}$, of the FGM plate with $h/a = 0.2$, $K_w = 100$, $K_s = 100$

supported FGM square plate resting on two parameter elastic foundation with $h/a = 0.2$, $K_w = 100$ and $K_s = 100$ as Thai and Choi (2011). Fig. 3 shows normalized fundamental frequency $\hat{\omega}$, of the plates for volume fraction exponent of, $n = 1$. This figure shows that, by using of only 5×5 node arrangement, the applied method has a very good accuracy and agreement with reported results by Thai and Choi (2011) in FGM plates. Also, the normalized fundamental frequency of this plate are presented in Table 2 for various values of h/a ($= 0.05, 0.1$ and 0.2) and elastic foundation coefficients. This table reveals that the applied method in has very good accuracy and agreement with the reported results by Thai and Choi (2011) and Baferani *et al.* (2011) especially in thinner plates.

The accuracy of applied mesh-free method in nanocomposite plates reinforced by straight CNT is examined too. Consider square simply supported UD and FG-CNTRC plates with CNT volume fraction, $V_{CN}^* = 0.17$ and values of b/h ($= 50, 20$ and 10). Table 3 compares normalized fundamental frequency $\hat{\omega}$, of the applied mesh-free method and FEM with FEM (based on FSDT) reported results by Zhu *et al.* (2012) and FEM (based on HSDT) reported results by Mehar *et al.* (2015). The results show a good agreement for both UD and FG nanocomposite reinforced by straight CNTs.

5.2 Free vibration analysis of FG-CNTRC plates

The effects of boundary conditions, plate thickness and coefficients of elastic foundation on the frequencies of FG-CNTRC plates are investigated in Table 4. This table shows the fundamental normalized frequency parameter, $\hat{\omega}$, for clamped and CSCS (C: clamped and S: simply supported) plates with CNT waviness, $w = 0.425$, aspect ratio, $AR = 1000$, and volume fraction, $V_{CN}^* = 0.17$. As observed, using of the elastic foundation increases the frequency parameters and frequency

parameters of clamped plates are bigger than frequencies of CSCS plates in all cases. Also, the frequency parameter is dramatically decreased by increasing of CNT waviness or by decreasing of the plate thickness. FG-X and FG-O for wavy CNT distribution show the best and worst reinforcement behavior in free vibration analysis, respectively.

Now, the effects of CNTs characteristics are investigated on the frequencies of the nanocomposite plates reinforced by wavy CNTs. Table 5 lists the normalized fundamental frequency, $\hat{\omega}$, for clamped square plates reinforced by wavy CNT resting on Winkler-Pasternak foundation with $K_w = 100$ and $K_s = 10$, and with ratio of plate thickness, $h/a = 0.1$. This table reveals that the effect of CNT waviness is more than CNT Volume fraction on the natural

Table 2 Comparison of the normalized fundamental frequency, $\hat{\omega}$, in simply supported square FGM plates

K_w	K_s	h/a	Method	$n = 0$	$n = 1$		
0	0	0.05	Present	0.0291	0.0222		
			Baferani et al. 2011	0.0291	0.0227		
			Thai and Choi 2011	0.0291	0.0222		
			Present	0.1135	0.0869		
			Baferani et al. 2011	0.1134	0.0891		
			Thai and Choi 2011	0.1135	0.0869		
		0.1	0.2	Present	0.4167	0.3216	
				Baferani et al. 2011	0.4154	0.3299	
				Thai and Choi 2011	0.4154	0.3207	
				0.05	Present	0.0411	0.0384
					Baferani et al. 2011	0.0411	0.0388
					Thai and Choi 2011	0.0411	0.0384
0.1	Present	0.1618	0.1519				
	Baferani et al. 2011	0.1619	0.1542				
	Thai and Choi 2011	0.1619	0.1520				
	0.2	Present	0.6167	0.5857			
		Baferani et al. 2011	0.6162	0.5978			
		Thai and Choi 2011	0.6162	0.5855			

Table 3 Comparison of the normalized fundamental frequency, $\hat{\omega}$, in simply supported square plates reinforced by straight CNTs ($V_{CN}^* = 0.17$)

b/h	UD				FG-X		
	Mesh-Free (31×31)	FEM & FSDT (31×31)	FEM & FSDT (Zhu et al. 2012)	FEM & HSDT (Mehar et al. 2015)	Mesh-Free (31×31)	FEM & FSDT (31×31)	FEM & FSDT (Zhu et al. 2012)
50	23.6323	23.6791	23.697	23.66561	28.3400	28.3891	28.413
20	21.5053	21.541	21.456	21.41301	24.8639	24.8973	24.764
10	17.0010	17.0189	16.815	16.83529	18.5240	18.5382	18.278

Table 4 Normalized fundamental frequency, $\hat{\omega}$, in clamped square FG-CNTRC plates with $w = 0.425$, $AR = 1000$ and $V_{CN}^* = 0.17$

B.C.	h/a	w	K _w	K _s	CNT Distribution			
					UD	FG-V	FG-X	FG-O
CCCC	0.1	0	0	0	0.2086	0.2045	0.2159	0.1974
			100	10	0.2153	0.2113	0.2224	0.2045
		0.425	0	0	0.1419	0.1434	0.1443*	0.1428
	100		10	0.1518	0.1532	0.1540**	0.1526	
	0.2	0.425	0	0	0.4302	0.4339	0.4352	0.4323
			100	10	0.4884	0.4817	0.4829	0.4804
CSCS	0.1	0.425	0	0	0.1161	0.1168	0.1202	0.1137
			100	10	0.1275	0.1281	0.1312	0.1253

*2nd frequency: 0.2638; 3rd frequency: 0.2709

** 2nd frequency: 0.2741; 3rd frequency: 0.2809

Table 5 Normalized fundamental frequency, $\hat{\omega}$, in clamped square FG-CNTRC plates with $K_w = 100$, $K_s = 10$ and $h/a = 0.1$

V _{CN} *	w	AR	CNT Distribution			
			UD	FG-V	FG-X	FG-O
0.12	0	400	0.1707	0.1674	0.1751	0.1628
		1000	0.1715	0.1684	0.1756	0.1641
	0.425	400	0.1285	0.1286	0.1284	0.1294
		1000	0.1290	0.1294	0.1288	0.1306
0.17	0	400	0.2142	0.2099	0.2217	0.2027
		1000	0.2153	0.2113	0.2224	0.2045
	0.425	400	0.1516	0.1527	0.1539	0.1518
		1000	0.1518	0.1532	0.1540	0.1526
0.28	0	400	0.2280	0.2282	0.2402	0.2201
		1000	0.2287	0.2292	0.2406	0.2215
	0.425	400	0.1528	0.1554	0.1594	0.1518
		1000	0.1528	0.1558	0.1595	0.1525

frequencies of the FG-CNTRC plates. Increasing of CNT volume fraction increases the frequency parameter but this effect is more considerable at small value of CNT volume fraction. Also, frequency parameter is increased by increasing of CNT aspect ratio, but CNT aspect ratio doesn't have a significant effect. Finally, it can be seen that, except in the plate with wavy CNT and $V_{CN}^* = 0.17$, X-CNTRC plates have the biggest values of frequencies parameters.

5.3 Forced vibration and resonance behavior in FG-CNTRC plates

In this section, forced vibration and resonance behavior of clamped square plates are

investigated. The plates subjected to a periodic uniform pressure load at top face as follows

$$P(t) = P_0 \sin(\omega_t t) \tag{41}$$

where ω_t is the frequency of time depended applied load. For resonance phenomenon, frequency of loading, ω_t , is equal to n^{th} natural frequency, ω_n . Figs. 4 and 5 illustrate the effects of loading frequency and elastic foundation on the forced vibration and resonance behavior of clamped X-CNTRC plates with $h/a = 0.1$, $b/a = 1$, $V_{CN}^* = 0.17$, $w = 0.425$ and $AR = 1000$ in two cases of $K_w = K_s = 0$ and $K_w = 100, K_s = 10$. Figs. 4 and 5 show time history of normalized central deflection, \hat{q} , of the plates in forced vibration and resonance analysis, respectively. In forced vibration analysis, the plates subjected to periodic loads with $\omega_t = \omega_0, 2\omega_0/3, \omega_0/3$, when $\omega_0 = 1500$ rad/s but for resonance phenomenon, the plate subjected to periodic loads with loading frequencies equal to

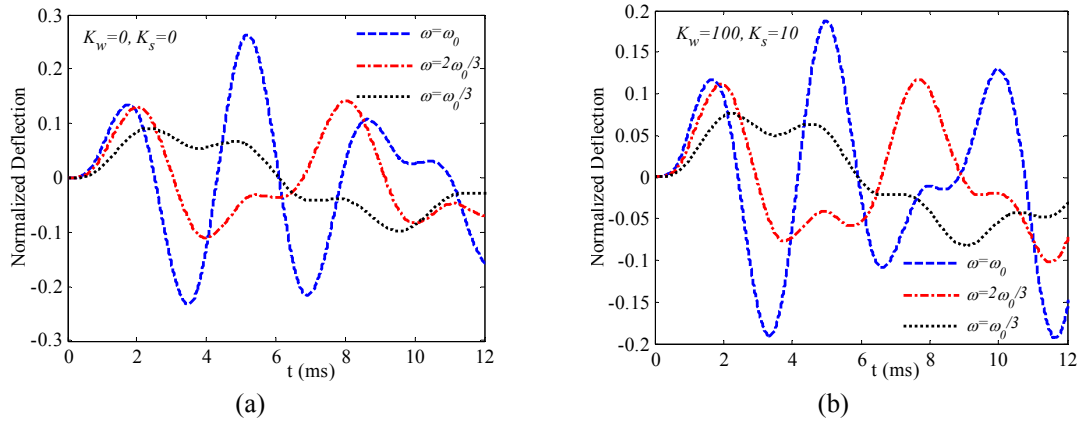


Fig. 4 Time history of normalized central deflections, \hat{q} , of clamped X-CNTRC plates with $b/a = 1$, $h/a = 0.1$, $V_{CN}^* = 0.17$, $w = 0.425$, $AR = 1000$ for (a) $K_w = 0, K_s = 0$; (b) $K_w = 100, K_s = 10$ (Forced Vibration)

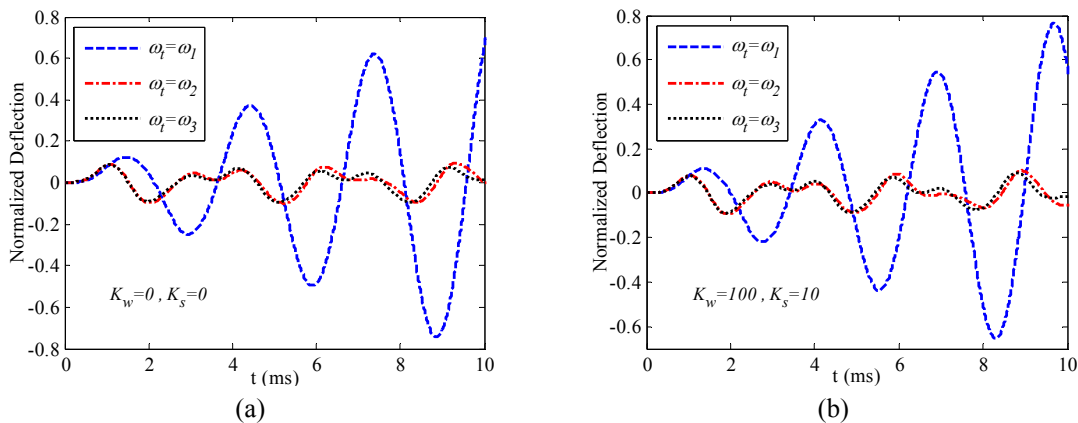


Fig. 5 Time history of normalized central deflections, \hat{q} , of clamped X-CNTRC plates with $b/a = 1$, $h/a = 0.1$, $V_{CN}^* = 0.17$, $w = 0.425$, $AR = 1000$ for (a) $K_w = 0, K_s = 0$; (b) $K_w = 100, K_s = 10$ (Resonance Phenomenon)

three first natural frequencies of the plates. It can be seen that elastic foundation decreased the amplitudes and increased speed of vibration the in both analyses. The resonance phenomenon is occurred only for loading with fundamental frequency.

Figs. 6 and 7 illustrate the effects of thickness and CNT distribution on the vibrational responses of clamped FG-CNTRC plates resting on the Winkler-Pasternak elastic foundation with $b/a = 1$, $V_{CN}^* = 0.17$, $w = 0.425$, $AR = 1000$, $K_w = 100$, $K_s = 10$ and with $h/a = 0.1$ and 0.2 . Figs. 6 and 7 show time history of normalized central deflection, \hat{q} , of the plates subjected to periodic load with loading frequency equal to $\omega_t = \omega_0$ (forced vibration) and $\omega_t = \omega_1$ (resonance), respectively. It can be seen that X-CNTRC plates have the biggest vibrational speeds and the smallest amplitudes of vibration while UD ones are in opposite points, for all cases. Increasing of the plate thickness increases the vibration amplitudes (by considering of Eq. (39)) and speeds especially for resonance responses.

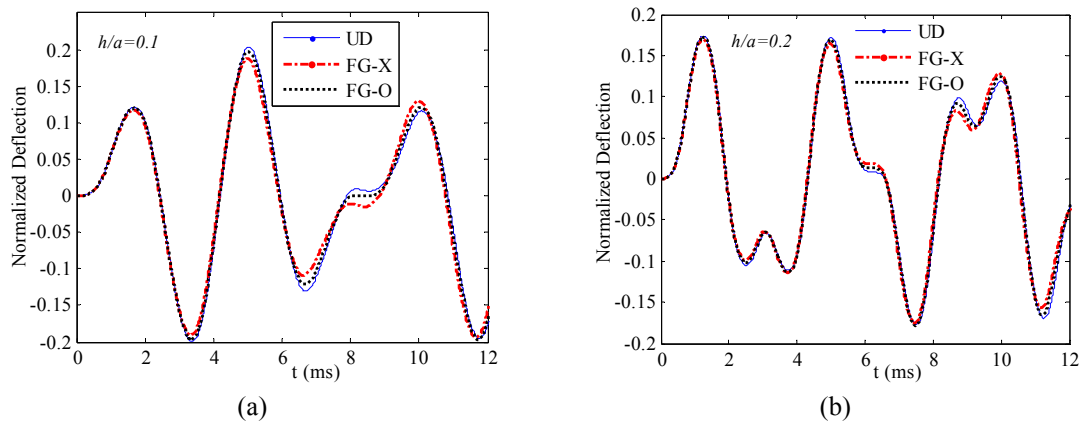


Fig. 6 Time history of normalized central deflections, \hat{q} , of clamped CNTRC plates with $\omega_t = \omega_0$, $b/a = 1$, $V_{CN}^* = 0.17$, $w = 0.425$, $AR = 1000$, $K_w = 100$, $K_s = 10$ for (a) $h/a = 0.1$; (b) $h/a = 0.2$ (Forced Vibration)

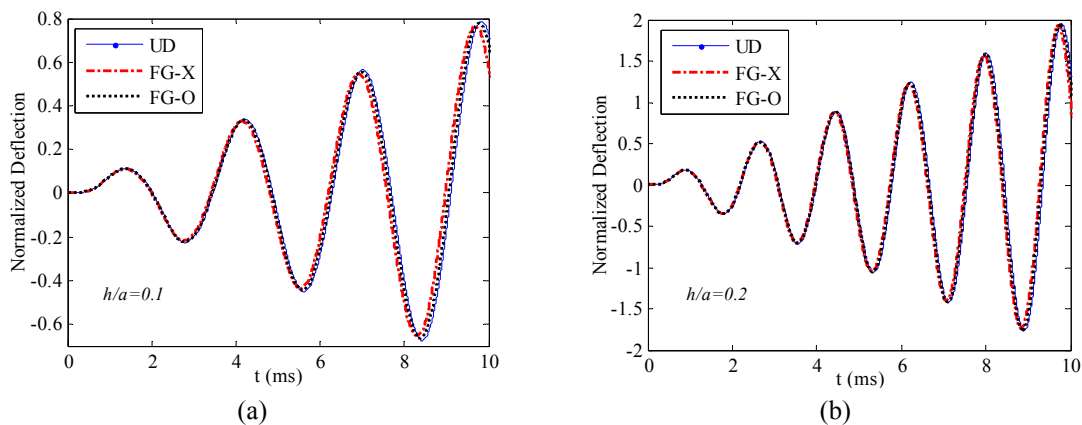


Fig. 7 Time history of normalized central deflections, \hat{q} , of clamped CNTRC plates with $\omega_t = \omega_0$, $b/a = 1$, $V_{CN}^* = 0.17$, $w = 0.425$, $AR = 1000$, $K_w = 100$, $K_s = 10$ for (a) $h/a = 0.1$; (b) $h/a = 0.2$ (Resonance Phenomenon)

Finally, the effects of CNT waviness and aspect ratio on the on the vibrational responses of FG-CNTRC plates resting on the Winkler-Pasternak elastic foundation are examined. Figs. 8 and 9 show forced vibration and resonance responses (time history of \hat{q}) for clamped X-CNTRC plates with $b/a = 1$, $h/a = 0.1$, $AR = 1000$, $K_w = 100$, $K_s = 10$ and with $w = 0$ and $w = 0.425$. It can be seen that increasing of the waviness increases vibrational amplitudes, changes profile of forced vibration responses and decreases the vibrational speeds in resonance responses. Also increasing of the CNT volume fraction increases vibrational speeds and decreases their amplitudes. These effects are more considerable in resonance responses.

5.2 Dynamic analysis of FG-CNTRC plates

In this section, dynamic behavior of FG-CNTRC plates resting on Winkler-Pasternak elastic foundation is investigated. The plates are subjected to a uniform impact load on the top face as follows

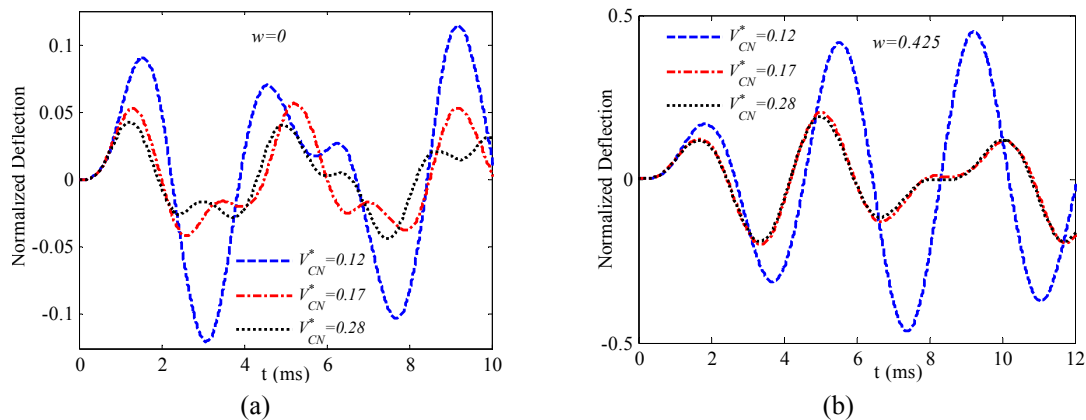


Fig. 8 Time history of normalized central deflections, \hat{q} , of clamped X-CNTRC plates with $\omega_t = \omega_0$, $b/a = 1$, $h/a = 0.1$, $AR = 1000$, $K_w = 100$, $K_s = 10$ for (a) $w = 0$; (b) $w = 0.425$ (Forced Vibration)

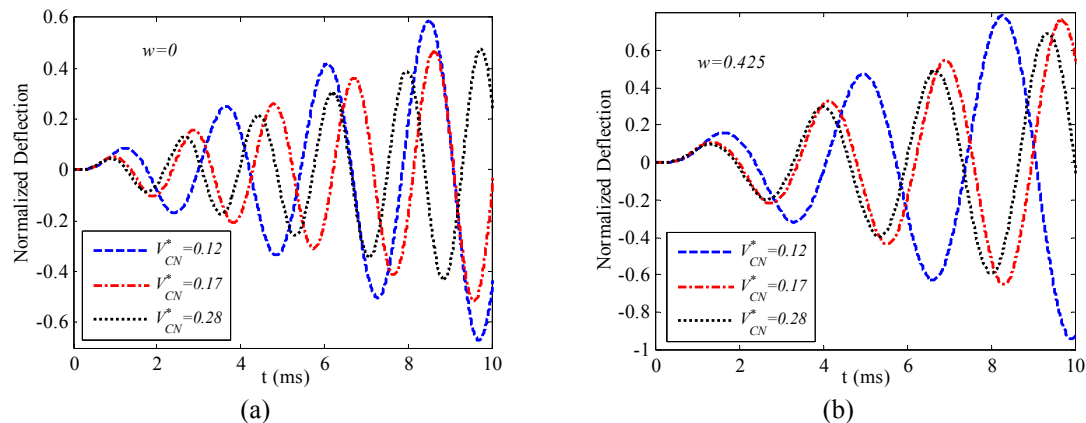


Fig. 9 Time history of normalized central deflections, \hat{q} , of clamped X-CNTRC plates with $\omega_t = \omega_0$, $b/a = 1$, $h/a = 0.1$, $AR = 1000$, $K_w = 100$, $K_s = 10$ for (a) $w = 0$; (b) $w = 0.425$ (Resonance Phenomenon)

$$\begin{aligned}
 P(t) &= P_0 \sin 4000\pi t & \text{for } t \leq 0.25 \text{ (ms)} \\
 P(t) &= 0 & \text{for } t > 0.25 \text{ (ms)}
 \end{aligned}
 \tag{42}$$

where $P_0 = -1e5 \text{ N/m}^2$ is the amplitude of the above half sine loading. In the following simulations, thickness plates is equal to $h = 0.1 \text{ m}$.

Fig. 10 show the effects of CNT distribution on the stress wave propagations and time history of deflection of clamped CNTRC plates with $h/a = 0.1$, $b/a = 1$, $K_w = 100$, $K_s = 10$, $V_{CN}^* = 0.17$, $w = 0.425$ and $AR = 1000$. Since Young's modules of CNT are greater than shear module, so values of normal stresses are much greater than shear stresses also UD and X-CNTRC plates have the biggest values of σ_{xx} and σ_{yy} , respectively. But, O and X-CNTRC plates have the minimum and maximum values of shear stresses, respectively. σ_{yz} has the biggest values of the shear stresses. Also, it can be seen that, CNT distribution doesn't have a significant effect on central deflections of the plates.

Fig. 11 show the effects of CNT volume fraction and waviness on the dynamic behavior of the clamped X-CNTRC plates with $h/a = 0.1$, $b/a = 1$, $K_w = 100$, $K_s = 10$ and $AR = 1000$. It can be seen that the normal stress at x direction has the maximum values of stresses. Increasing of waviness index increases the values of deflection and stresses except for σ_{xz} (at low value of CNT volume) and σ_{xx} . Also, increasing of the CNT volume fraction increases the values of stresses in all cases (except for σ_{xx} in plates with different values of waviness index) and decreases the values of deflection in wavy CNT-reinforced plates.

Fig. 12 show the effects of Winkler-Pasternak elastic foundation coefficients on the dynamic behavior of clamped X-CNTRC plates with $h/a = 0.1$, $b/a = 1$, $V_{CN}^* = 0.17$, $w = 0.425$ and $AR = 1000$. It can be seen that using of elastic foundation decreases the values of stresses and deflection in all cases, while the effect of shear coefficient, K_s , is more than the normal coefficient, K_w .

Fig. 13 show time histories of σ_{xx} (in-plane) and σ_{zz} (out-plane) at top, mid and bottom planes ($z = -h, 0, h$) of clamped X-CNTRC plates with $h/a = 0.1$, $b/a = 1$, $K_w = 100$, $K_s = 10$, $V_{CN}^* = 0.28$, $w = 0.425$ and $AR = 1000$. It can be seen that the plate at $z = 0$ almost senses no in-plane stresses while top and bottom planes sense the same in-plane stresses with different sign. But, the plates sense out-plane stresses at $z = 0$ and their values are less than the values of stresses at $z = -h$ and h .

6. Conclusions

In this paper, dynamic responses of nanocomposite plates reinforced by wavy CNTs resting on Winkler-Pasternak elastic foundation were investigated by a mesh-free method based on FSDT. The plates were assumed subjected to periodic or impact loading for vibration or stress wave propagation analysis, respectively. CNT distribution was assumed to be functionally graded along the plate thickness. So, the effects of CNTs aspect ratio, waviness index, distribution pattern and volume fraction, and also elastic foundation coefficients, plate thickness and time depended loading were examined on the vibrational and dynamic behavior of the plates. The following results were obtained:

- The developed mesh-free method has an excellent convergence and accuracy for dynamic analysis of the plates.
- Using of the elastic foundation increases the frequency parameters of FG-CNTRC plates.
- The frequency parameter is dramatically decreased by increasing of CNT waviness or by

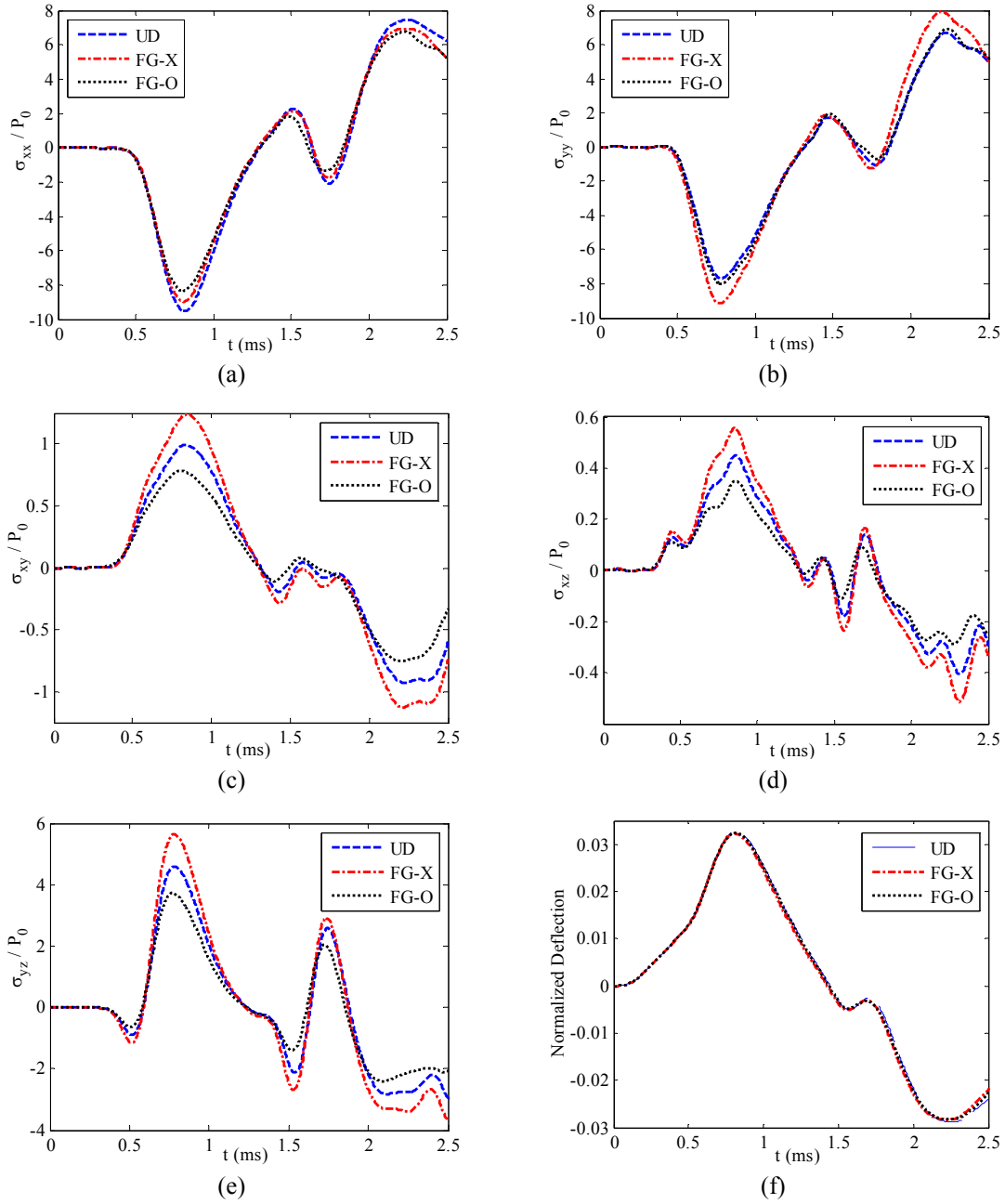


Fig. 10 Time history of (a) σ_{xx} ; (b) σ_{yy} ; (c) σ_{xy} ; (d) σ_{xz} ; (e) σ_{yz} ; and (f) \hat{q} , at top face of clamped CNTRC plates with $h/a = 0.1$, $b/a = 1$, $V_{CN}^* = 0.17$, $w = 0.425$, $AR = 1000$, $K_w = 100$, $K_s = 10$

- decreasing of the plate thickness
- The effect of CNT waviness is more than CNT Volume fraction on the natural frequencies of the FG-CNTRC plates.
- The resonance phenomenon is accrued only for loading with fundamental frequency.

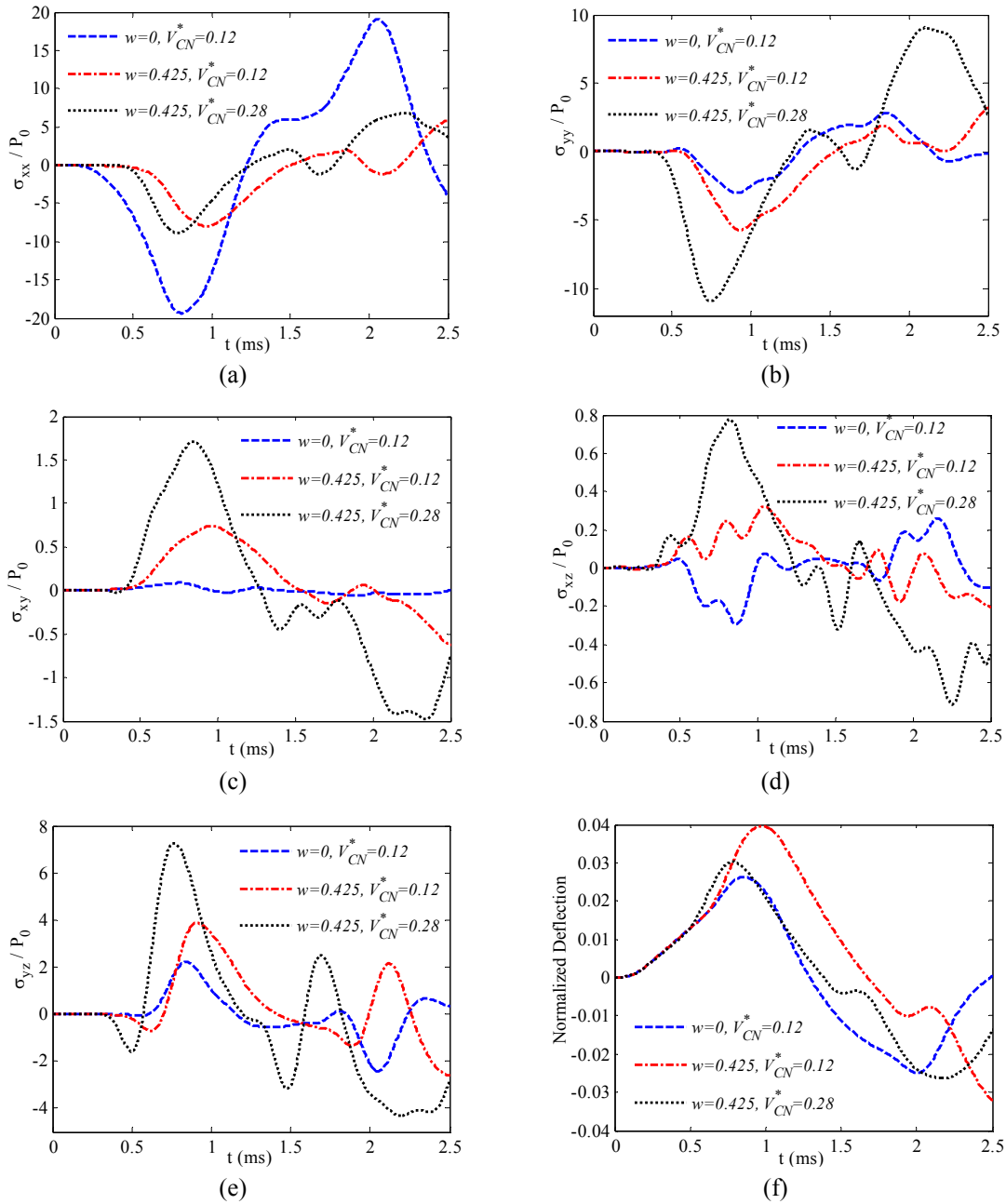


Fig. 11 Time time history of (a) σ_{xx} ; (b) σ_{yy} ; (c) σ_{xy} ; (d) σ_{xz} ; (e) σ_{yz} ; and (f) \hat{q} , at top face of clamped X-CNTRC plates with $h/a = 0.1$, $b/a = 1$, $AR = 1000$, $K_w = 100$, $K_s = 10$

- Increasing of CNT waviness increases vibrational amplitudes, changes profile of forced vibration responses and decreases the vibrational speeds in resonance responses.
- Increasing of the CNT volume fraction increases vibrational speeds and decreases their amplitudes.

- The values of normal stresses are more than shear stresses.
- In most cases, increasing of waviness index increases the values of deflection and stresses. Also, increasing of the CNT volume fraction increases the values of stresses and decreases the values of deflection in wavy CNT-reinforced plates.

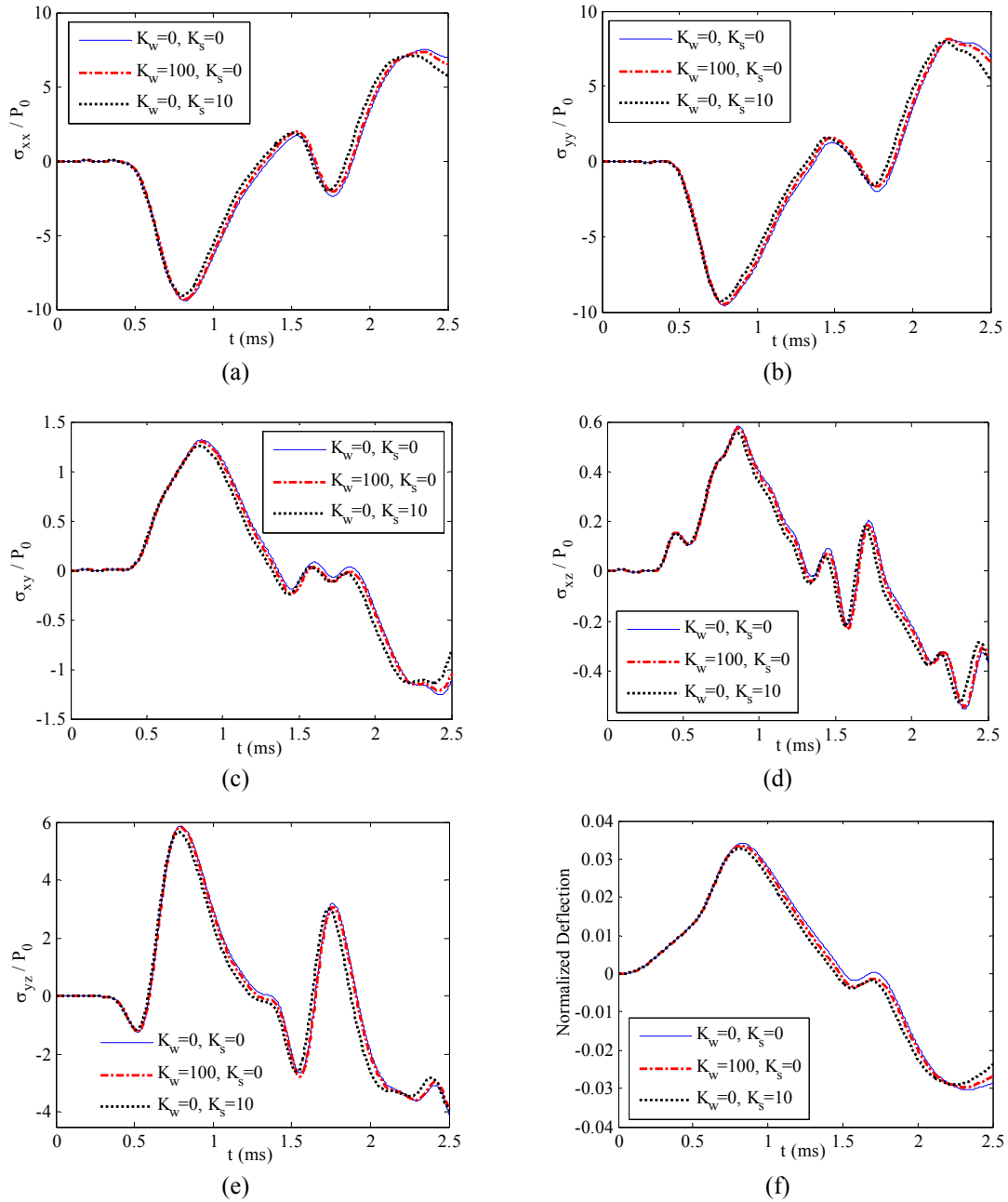


Fig. 12 Time time history of (a) σ_{xx} ; (b) σ_{yy} ; (c) σ_{xy} ; (d) σ_{xz} ; (e) σ_{yz} ; and (f) \hat{q} , at top face of clamped X-CNTRC plates with $h/a = 0.1$, $b/a = 1$, $V_{CN}^* = 0.17$, $w = 0.425$, $AR = 1000$

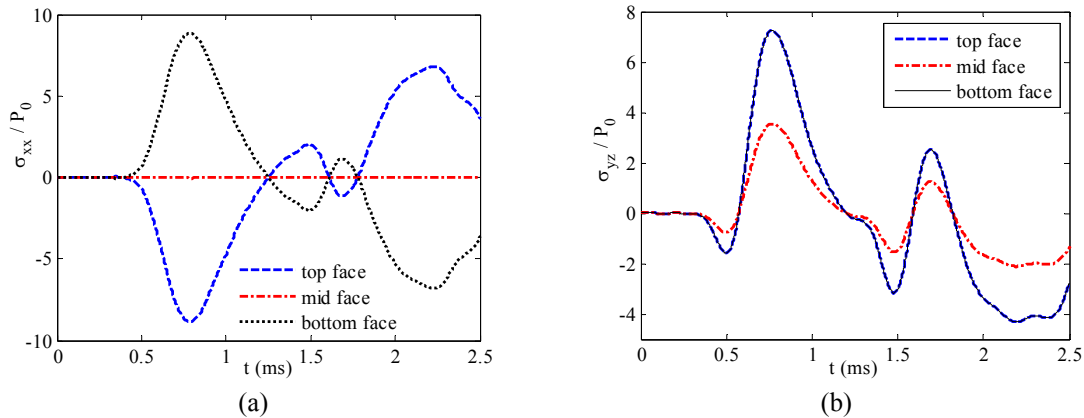


Fig. 13 Time history of (a) σ_{xx} ; and (b) σ_{yz} in clamped X-CNTRC plates with $h/a = 0.1$, $b/a = 1$, $V_{CN}^* = 0.28$, $w = 0.425$, $AR = 1000$, $K_w = 100$, $K_s = 10$

References

- Ansari, R. and Arjangpay, A. (2014), "Nanoscale vibration and buckling of single-walled carbon nanotubes using the meshless local Petrov–Galerkin method", *Physica E*, **63**, 283-292.
- Ansari, R., Hasrati, E., Faghieh Shojaei, M., Gholami, R. and Shahabodini, A. (2015), "Forced vibration analysis of functionally graded carbon nanotube-reinforced composite plates using a numerical strategy", *Physica E*, **69**, 294-305.
- Baferani, A.H., Saidi, A.R. and Ehteshami, H. (2011), "Accurate solution for free vibration analysis of functionally graded thick rectangular plates resting on elastic foundation", *Compos. Struct.*, **93**(7), 1842-1853.
- Efraim, E. and Eisenberger, M. (2007), "Exact vibration analysis of variable thickness thick annular isotropic and FGM plates", *J. Sound Vib.*, **299**(4-5), 720-738.
- Fan, Y. and Wang, H. (2016), "The effects of matrix cracks on the nonlinear bending and thermal postbuckling of shear deformable laminated beams containing carbon nanotube reinforced composite layers and piezoelectric fiber reinforced composite layers", *Compos. Part B*, **106**, 28-41.
- Fantuzzi, N., Tornabene, F., Bacciocchi, M. and Dimitri, R. (2016), "Free vibration analysis of arbitrarily shaped functionally graded Carbon Nanotube-reinforced plates", *Compos. Part B*. [In Press]
DOI: <http://dx.doi.org/10.1016/j.compositesb.2016.09.021>
- Ferreira, A.J.M., Castro, L.M.S. and Bertoluzza, S. (2009), "A high order collocation method for the static and vibration analysis of composite plates using a first-order theory", *Compos. Struct.*, **89**(3), 424-432.
- Fidelus, J.D.D., Wiesel, E., Gojny, F.H.H., Schulte, K. and Wagner, H.D.D. (2005), "Thermo-mechanical properties of randomly oriented carbon/epoxy nanocomposites", *Compos. A Appl. Sci. Manuf.*, **36**(11), 1555-61.
- Han, Y. and Elliott, J. (2007), "Molecular dynamics simulations of the elastic properties of polymer/ carbon nanotube composites", *Comput. Mater. Sci.*, **39**(2), 315-323.
- Hedayati, H. and Sobhani Aragh, B. (2012), "Influence of graded agglomerated CNTs on vibration of CNT-reinforced annular sectorial plates resting on Pasternak foundation", *Appl. Math. Comput.*, **218**(17), 8715-8735.
- Iijima, S. (1991), "Helical microtubes of graphitic carbon", *Nature*, **354**, 56-58.
- Iijima, S. and Ichihashi, T. (1993), "Single-shell carbon nanotubes of 1-nm diameter", *Nature*, **363**, 603-605.
- Jafari Mehrabadi, S. and Sobhani Aragh, B. (2014), "Stress analysis of functionally graded open cylindrical shell reinforced by agglomerated carbon nanotubes", *Thin-Wall. Struct.*, **80**, 130-141.
- Jam, J.E., Pourasghar, A. and Kamarian, S. (2012), "The effect of the aspect ratio and waviness of CNTs on

- the vibrational behavior of functionally graded nanocomposite cylindrical panels”, *Polym. Compos.*, **33**(11), 2036-2044.
- Kaci, A., Tounsi, A., Bakhti, K. and Bedia, E.A.A. (2012), “Nonlinear cylindrical bending of functionally graded carbon nanotube-reinforced composite plates”, *Steel Compos. Struct., Int. J.*, **12**(6), 491-504.
- Kamarian, S., Pourasghar, A. and Yas, M.H. (2013), “Eshelby-Mori-Tanaka approach for vibrational behavior of functionally graded carbon nanotube-reinforced plate resting on elastic foundation”, *J. Mech. Sci. Technol.*, **27**(11), 3395-3401.
- Kamarian, S., Salim, M., Dimitri, R. and Tornabene, F. (2016), “Free vibration analysis of conical shells reinforced with agglomerated carbon nanotubes”, *Inter. J. Mech. Sci.*, **108-109**, 157-165.
- Kundalwal, S.I. and Ray, M.C. (2013), “Effect of carbon nanotube waviness on the elastic properties of the fuzzy fiber reinforced composites”, *ASME J. Appl. Mech.*, **80**(2), 021010.
- Lancaster, P. and Salkauskas, K. (1981), “Surface generated by moving least squares methods”, *Math. Comput.*, **37**, 141-158.
- Lei, Z.X., Liew, K.M. and Yu, J.L. (2013a), “Buckling analysis of functionally graded carbon nanotube-reinforced composite plates using the element-free kp-Ritz method”, *Compos. Struct.*, **98**, 160-168.
- Lei, Z.X., Liew, K.M. and Yu, J.L. (2013b), “Free vibration analysis of functionally graded carbon nanotube-reinforced composite plates using the element-free kp-Ritz method in thermal environment”, *Compos. Struct.*, **106**, 128-138.
- Lei, Z.X., Zhang, L.W., Liew, K.M. and Yu, J.L. (2016), “Dynamic stability analysis of carbon nanotube-reinforced functionally graded cylindrical panels using the element-free kp-Ritz method”, *Compos. Struct.*, **113**, 328-338.
- Liew, K.M., Lei, Z.X. and Zhang, L.W. (2015), “Mechanical analysis of functionally graded carbon nanotube reinforced composites, A review”, *Compos. Struct.*, **120**, 90-97.
- Martone, A., Faiella, G., Antonucci, V., Giordano, M. and Zarrelli, M. (2011), “The effect of the aspect ratio of carbon nanotubes on their effective reinforcement modulus in an epoxy matrix”, *Compos. Sci. Technol.*, **71**(8), 1117-1123.
- Meguid, S.A. and Sun, Y. (2004), “On the tensile and shear strength of nano-reinforced composite interfaces”, *Mater. Des.*, **25**(4), 289-296.
- Mehar, K., Panda, S.K., Dehengia, A. and Ranjan Kar, V. (2015), “Vibration analysis of functionally graded carbon nanotube reinforced composite plate in thermal environment”, *J. Sand. Struct. Mater.*, **18**(2), 151-173.
- Mindlin, R.D. (1951), “Influence of rotatory inertia and shear on flexural motions of isotropic, elastic plates”, *J. Appl. Mech.*, **18**, 31-38.
- Moradi-Dastjerdi, R. (2016), “Wave propagation in functionally graded composite cylinders reinforced by aggregated carbon nanotube”, *Struct. Eng. Mech., Int. J.*, **57**(3), 441-456.
- Moradi-Dastjerdi, R. and Pourasghar, A. (2016), “Dynamic analysis of functionally graded nanocomposite cylinders reinforced by wavy carbon nanotube under an impact load”, *J. Vib. Control*, **22**(4), 1062-1075.
- Moradi-Dastjerdi, R., Foroutan, M. and Pourasghar, A. (2013a), “Dynamic analysis of functionally graded nanocomposite cylinders reinforced by carbon nanotube by a mesh-free method”, *Mater. Des.*, **44**, 256-266.
- Moradi-Dastjerdi, R., Foroutan, M., Pourasghar, A. and Sotoudeh-Bahreini, R. (2013b), “Static analysis of functionally graded carbon nanotube-reinforced composite cylinders by a mesh-free method”, *J. Reinf. Plast. Compos.*, **32**(9), 593-601.
- Moradi-Dastjerdi, R., Pourasghar, A., Foroutan, M. and Bidram, M. (2014), “Vibration analysis of functionally graded nanocomposite cylinders reinforced by wavy carbon nanotube based on mesh-free method”, *J. Compos. Mater.*, **48**, 1901-1913.
- Natarajan, S., Haboussi, M. and Manickam, G. (2014), “Application of higher-order structural theory to bending and free vibration analysis of sandwich plates with CNT reinforced composite face sheets”, *Compos. Struct.*, **113**, 197-207.
- Qian, L.F., Batra, R.C. and Chen, L.M. (2004), “Static and dynamic deformations of thick functionally graded elastic plates by using higher-order shear and normal deformable plate theory and meshless local

- Petrov–Galerkin method”, *Compos. Part B*, **35**(6-8), 685-697.
- Reddy, J.N. (1984), “A simple higher order theory for laminated composite plates”, *J. Appl. Mech.*, **51**(4), 745-752.
- Reddy, J.N. (2004), *Mechanics of Laminated Composite Plates and Shells: Theory and Analysis*, CRC.
- Reissner, E. (1945), “The effect of transverse shear deformation on the bending of elastic plates”, *J. Appl. Mech.*, **12**, 69-72.
- Selmi, A., Friebel, C., Doghri, I. and Hassis, H. (2007), “Prediction of the elastic properties of single walled carbon nanotube reinforced polymers: A comparative study of several micromechanical models”, *Compos. Sci. Technol.*, **67**(10), 2071-2084.
- Shams, S. and Soltani, B. (2015), “The effects of carbon nanotube waviness and aspect ratio on the buckling behavior of functionally graded nanocomposite plates using a meshfree method”, *Polymer Compos.*
DOI: 10.1002/pc.23814
- Shen, H.S. (2009), “Nonlinear bending of functionally graded carbon nanotube- reinforced composite plates in thermal environments”, *Compos. Struct.*, **91**(1), 9-19.
- Sobhani Aragh, B., Nasrollah Barati, A.H. and Hedayati, H. (2012), “Eshelby–Mori–Tanaka approach for vibrational behavior of continuously graded carbon nanotube-reinforced cylindrical panels”, *Compos. Part B*, **43**(4), 1943-1954.
- Song, Y.S. and Youn, J.R. (2006), “Modeling of effective elastic properties for polymer based carbon nanotube composites”, *Polymer*, **47**(5), 1741-1748.
- Thai, H.T. and Choi, D.H. (2011), “A refined plate theory for functionally graded plates resting on elastic foundation”, *Compos. Sci. Technol.*, **71**(16), 1850-1858.
- Thai, H.T. and Choi, D.H. (2012), “An efficient and simple refined theory for buckling analysis of functionally graded plates”, *Appl. Math. Model.*, **36**(3), 1008-1022.
- Tornabene, F., Fantuzzi, N., Baccocchi, M. and Viola, E. (2016), “Effect of agglomeration on the natural frequencies of functionally graded carbon nanotube-reinforced laminated composite doubly-curved shells”, *Compos. Part B*, **89**, 187-218.
- Yas, M.H. and Sobhani Aragh, B. (2010), “Free vibration analysis of continuous grading fiber reinforced plates on elastic foundation”, *Inter. J. Eng. Sci.*, **48**(12), 1881-1895.
- Zhang, L.W., Lei, Z.X. and Liew, K.M. (2015a), “An element-free IMLS-Ritz framework for buckling analysis of FG–CNT reinforced composite thick plates resting on Winkler foundations”, *Eng. Anal. Bound. Elem.*, **58**, 7-17.
- Zhang, L.W., Song, Z.G. and Liew, K.M. (2015b), “Nonlinear bending analysis of FG-CNT reinforced composite thick plates resting on Pasternak foundations using the element-free IMLS-Ritz method”, *Compos. Struct.*, **128**, 165-175.
- Zhu, P., Lei, Z.X. and Liew, K.M. (2012), “Static and free vibration analyses of carbon nanotube-reinforced composite plates using finite element method with first order shear deformation plate theory”, *Compos. Struct.*, **94**(4), 1450-1460.